Korean Journal of Remote Sensing, Vol.20, No.3, 2004, pp.175~188

Comparison of Remote Sensing and Crop Growth Models for Estimating Within-Field LAI Variability

Suk-Young Hong*, Kenneth A. Sudduth, Newell R. Kitchen**, Clyde W. Fraisse***, Harlan L. Palm****, and William J. Wiebold*****

National Institute of Agricultural Science and Technology, Rural Development Administration*
Cropping Systems and Water Quality Research Unit, USDA-ARS, Columbia, Missouri, USA**
Agricultural and Biological Engineering Department, University of Florida, Gainesville, Florida, USA***
Agronomy Department, University of Missouri, Columbia, Missouri, USA****

Abstract : The objectives of this study were to estimate leaf area index (LAI) as a function of image-derived vegetation indices, and to compare measured and estimated LAI to the results of crop model simulation. Soil moisture, crop phenology, and LAI data were obtained several times during the 2001 growing season at monitoring sites established in two central Missouri experimental fields, one planted to corn (*Zea mays* L.) and the other planted to soybean (*Glycine max* L.). Hyper- and multi-spectral images at varying spatial and spectral resolutions were acquired from both airborne and satellite platforms, and data were extracted to calculate standard vegetative indices (normalized difference vegetative index, NDVI; ratio vegetative index, RVI; and soil-adjusted vegetative index, SAVI). When comparing these three indices, regressions for measured LAI were of similar quality (r^2 = 0.59 to 0.61 for corn; r^2 = 0.66 to 0.68 for soybean) in this single-year dataset. CERES(Crop Environment REsource Synthesis)-Maize and CROPGRO-Soybean models were calibrated to measured soil moisture and yield data and used to simulate LAI over the growing season. The CERES-Maize model over-predicted LAI at all corn monitoring sites. Simulated LAI from CROPGRO-Soybean was similar to observed and image-estimated LAI for most soybean monitoring sites. These results suggest crop growth model predictions might be improved by incorporating image-estimated LAI. Greater improvements might be expected with corn than with soybean.

Key Words : Precision Farming, LAI, NDVI, Remote Sensing, Crop Models.

1. Introduction

Crop yield is a function of complex interactions of biotic and abiotic factors, including crop management (e.g., fertility, variety, and seeding rate), soil and field characteristics (e.g., drainage, topography, and soil water holding capacity), and weather conditions (e.g., temperature, precipitation, and light use efficiency). Understanding the relationship of crop yield to other spatial factors is needed to develop appropriate site-

Received 3 May 2004; Accepted 4 June 2004.

specific crop management (SSCM) systems. Crop production varies not only spatially but also temporally. High-producing areas of a field during "dry" years can be low-producing areas in "wet" years (Colvin *et al.*, 1997; Wang *et al.*, 2003).

Crop modeling has been applied at various scales in agriculture, from precision farming, to farm planning, to watershed or regional policy development. CROPGRO-Soybean (Hoogenboom *et al.*, 1994) and CERES-Maize (Jones and Kiniry, 1986) are process-oriented models that compute growth, development, and yield on homogeneous units from field to regional scales. Although crop modeling is a promising tool for simulating yield and yield-limiting factors, a large amount of input data is necessary to accurately predict spatial variations, and the cost for measuring dense spatial data sets is high. To quantify in-field spatial variations using crop models, reliable and cost-effective techniques must be developed to parameterize crop models across a field with high spatial resolution.

Remote sensing technologies for precision agriculture are used to detect and quantify various field conditions including crops, soils, water, and climate for immediate and future management decisions. Functional relations have been developed between remote spectral observations and crop characteristics such as above-ground net production (ANP) (Hong *et al.*, 1997), yield, fractional photosynthetically active radiation (FPAR), leaf area index (LAI) (Wiegand *et al.*, 1991; Thenkabail *et al.*, 2000), shoot population (Wood *et al.*, 2003), and soil properties including soil texture and fertility (Thomasson *et al.*, 2001; Hong *et al.*, 2001).

Vegetation indices (VI) are dimensionless, radiometric measures that function as indicators of relative abundance and activity of green vegetation. A vegetation index should maximize sensitivity to plant biophysical parameters, normalize or model external effects such as sun angle, viewing angle, and the atmosphere, and normalize internal effects such as canopy background variations. In spectral signature analysis by remote sensing, vegetation indices that combine red and near-infrared bands are widely used for estimating the vitality and the productivity of vegetation. The cellular structure of leaf mesophyll strongly scatters and reflects near-infrared energy. In the visible region, vegetation looks dark on the imagery because of the high absorption of pigments such as chlorophylls and xanthophylls. Although these physical bases explain their function, vegetation indices are generally based on empirical evidence, not on basic biology, chemistry or physics.

Leaf area index (LAI) was first introduced by Watson (1947) and defined as the ratio of leaf area to a given unit of land area, a ratio that is functionally linked to spectral reflectance. LAI is important in explaining the ability of the crop to intercept solar energy and in understanding the impact of crop management practices. Many have attempted to develop relationships between vegetation indices and LAI and have discussed their potential and limitations (Baret and Guyot, 1991; Wiegand *et al.*, 1991; Thenkabail *et al.*, 2000).

A number of attempts have been made to link remote sensing data to crop simulation models as direct inputs or for minimizing differences between predicted and measured values. Data used for model linkage have included 20- to 30-m resolution multispectral images (Wiegand *et al.*, 1986; Maas, 1988; Moulin *et al.*, 1998) for large-area crop condition assessment, and remotely-sensed canopy temperature for canopy transpiration (Inoue, 2001). In spite of the various studies conducted on integrating models and remote sensing data, spatial scale issues and integration methodologies are still uncertain and require further investigation.

The objective of this study was to estimate leaf area index (LAI) as a function of image-derived vegetation indices, and to compare measured and estimated LAI to the results of crop model simulation.

2. Spatial Data Collection, Modeling, and Image Analysis

1) Study Sites

Data were collected on two fields (Field A, 36 ha and Field B, 13 ha) located within 3 km of each other near Centralia, in central Missouri (39.2 N, 92.1 W), USA. The soils found at these sites are characterized as claypan soils (fine, montmorillonotic, mesic, Udollic Ocharaqualfs, and Albaquic Hapludalfs). These soils are poorly drained and have a restrictive, high-clay layer (the claypan) occurring below the topsoil. Because of extensive weathering, the claypan soil is usually low in natural fertility and pH. Plant available water from the claypan soil is low because a large portion of the stored water is retained with the clay at the wilting point.

Mapped data available for field characterization included a detailed, first-order soil survey, topographic maps, topsoil depth, and historical grain yield. Based on previous work (Doolittle *et al.*, 1994; Kitchen *et al.*, 1999), topsoil thickness above the claypan was estimated from soil electrical conductivity measured using a commercial electromagnetic induction sensor. Yield maps were available for the years beginning in 1993 (Field A) or 1996 (Field B). The selection of within-field monitoring sites for this study was based on this existing topography, topsoil depth, and historic yield information (Fraisse *et al.*, 2001). Topsoil depth and landscape position influence water holding capacity and water flow within the fields, having a direct impact on crop yield. The main goal was to select enough sites to adequately characterize the yield variability measured in the fields. Seven monitoring sites in Field A (Sites 101-107) and five in Field B (Sites 201-205) were selected to represent the range of variability present in the fields. Two monitoring sites, one in Field A (102) and the other in Field B (203), were located in depositional areas and were problematic in "wet" years due to surface and subsurface run-on from the upper parts of the fields. These areas generally exhibited above average yields in "dry" years, and, mainly due to reductions in stand, low yields in "wet" years.

Data for this study were collected in 2001. Field A was planted to corn on April 28 (76 cm row spacing, 63,000 seeds/ha) and Field B was planted to soybean on June 18 (19 cm row spacing, 490,000 seeds/ha). Field A was managed with minimum tillage, while Field B was managed with no-tillage. Harvest was on September 20 for Field A and October 17 for Field B.

2) Experimental Measurements

Neutron access tubes were installed at each site in the two fields for root zone soil moisture monitoring during the growing season. Soil moisture readings by neutron probe were made to determine the soil water content every other week at selected depths (15-, 30-, 45-, 60-, 80-, 100-, and 120-cm). Weather data needed for crop modeling, including solar radiation, maximum and minimum daily air temperature, and precipitation, were collected by an automated weather station located at Field A. A second rain gage was installed at Field B, providing precipitation data specific to each field.

A hydraulic core sampler was used for soil sampling at each site for both fields in November 1999. Cores were subsampled by horizon for bulk density and soil texture analysis. Bulk density was measured by the core method and soil textural composition was analyzed using the pipet method. The drained lower and upper limits were estimated using the Leaching Estimation and Chemistry describing water regime (LEACHW) model (Rawls and Brakensiek, 1985) available in SOILPAR (Soil Parameter Estimator) v1.0 (Donatelli *et al.*, 1996). The remaining soil properties used as input parameters for the crop growth models were taken from United States Department of Agriculture Natural Resources Conservation Service (USDA-NRCS) first order soil surveys conducted on Field A in 1997 and on Field B in

2000.

Destructive crop sampling for LAI and dry weight was carried out with a 1-m row section for corn (76-cm row spacing) and three 1-meter row sections for soybean (19-cm row spacing). Corn measurements were obtained on day of year (DOY) 177, 199, 218, and 240, while soybean measurements were obtained on DOY 211 and 229. Leaf area was measured with a LI-COR[1)] leaf area meter (LI-3100), where the projected image of a leaf sample traveling under a fluorescent light source is reflected by a system of mirrors to a solid-state scanning camera. Hatfield *et al.* (1976) reported that measurement error with this type of area meter is generally less than 2 %.

3) Crop Growth Models

The CERES-Maize and CROGRO-Soybean models included in the Decision Support System for Agrotechnology Transfer (DSSAT) v.3.5 software package (Hoogenboom *et al.*, 1994) were used to simulate crop growth. Both models are mechanistic process-based models that predict daily photosynthesis, growth, and partitioning in response to daily weather inputs, soil traits, crop management, and genetic traits. Fraisse *et al.* (2001) and Wang *et al.* (2003) evaluated the CERES-Maize and CROPGRO-soybean models for simulating site-specific crop development and yield on Missouri claypan soils.

Matthews and Blackmore (1997) suggested a framework for analyzing the factors causing spatial variation in crop yields following a hierarchical system of production levels: 1) potential production; 2) water-limited production; 3) nutrient-limited production; 4) production limited by weeds, pests, and diseases. Our study limited crop modeling to the second production level, in which weather data and soil water characteristics were used as the main input state variables.

4) Image Processing and Analysis

Airborne and IKONOS satellite images were acquired several times both for Field A and Field B during the 2001 cropping season as exampled in Table 1. The aerial hyperspectral images were collected using a pushbroom prism-grating scanner (RDACSH3; Real Time Digital Airborne Camera System H3) operated by Spectral Visions Midwest that included 120 bands from 471 nm to 828 nm (3-nm interval) with a spatial resolution of 1 m (Mao, 2000). The aerial multispectral sensor (RDACS; 1 to 1.3-m spatial resolution) included green (520-600 nm), red (630-690nm), and near-infrared (NIR; 760-790 nm) bands. The satellite multispectral sensor (IKONOS; 4-m spatial resolution) provided data in the same green, red, and NIR wavelength ranges.

Geometric distortion was observed in many airborne

1) Mention of trade names or commercial products is solely for the purpose of providing specific information and does not imply recommendation or endorsement by the authors or their organizations.

Table 1. Image acquisition information, 2001.

Sensor	Spatial Resolution(m)	Acquisition Date		
		Field A	Field B	Day of Year
Airborne hyperspectral	1	June 15		166
IKONOS multispectral	4	July 5	July 5	186
Airborne multispectral	1.3	July 15	July 15	196
Airborne multispectral	1	Aug. 6		218
IKONOS multispectral	4		Aug. 7	219
IKONOS multispectral	4	Aug. 29	Aug. 29	241
Airborne hyperspectral	1	Sep. 5	Sep. 5	248

images, probably due to aircraft attitude change during image acquisition. We applied a rubber sheeting model using piecewise polynomials for image rectification (Hong *et al.*, 2001). Data used for geo-referencing included accurate surveyed field boundary vector data, six ground control points per field, and a resolution-merged IKONOS image with a spatial resolution of 1 m.

For radiometric calibration of airborne images, chemically-treated reference tarps were used. These tarps included eight known reflectance levels from 2% to 88%, a range wide enough to represent all field surface reflection conditions. The tarps were placed at Field A during flights and reflectance data were retrieved from the images using linear regression models. The same regression models were used to convert digital numbers to reflectance for Field B images. The airborne multispectral image taken on July 15 did not have tarps and was used for data analysis without radiometric calibration. IKONOS imagery was radiometrically corrected by the image provider to adjust brightness and contrast to compensate for sensor sensitivity changes.

The areas for extracting VIs from the images were selected coincident with the hand-harvested areas for modeling (5m by 5m) with the assumption that crop samples obtained for model LAI estimation represented crop growth in the monitoring areas. The indices used for deriving image-based LAI values were NDVI (Normalized Difference Vegetation Index=$(\lambda_{NIR}-\lambda_R)/(\lambda_{NIR}+\lambda_R)$; Rouse *et al.*, 1973), RVI (Ratio Vegetation Index=λ_{NIR}/λ_R; Jordan, 1969), and SAVI (Soil Adjusted Vegetation Index=$(\lambda_{NIR}-\lambda_R)/(\lambda_{NIR}+\lambda_R+L)\times(1+L)$; Huete, 1988). To calculate VIs from hyperspectral images, the wavelengths selected were 681 nm for red, and 786 nm for NIR. These were selected based on spectral characteristics, pigment absorption, and our previous research (Hong *et al.*, 2001). Before extracting data for VI calculation, the MNF (Minimum Noise Fraction) transformation (Green *et al.*, 1988) was used to reduce random noise. The MNF transformation is a two-step principal component transformation in which the noise is decorrelated during the first step using the noise covariance matrix to provide unit variance and no band-to-band correlation. Then the second principal component transformation results in a data set where components are ranked in terms of noise equivalent radiance.

3. Results and Discussions

1) Leaf Area Index Estimation Using Remote Sensing

Image-derived NDVI was compared with observed LAI both for corn in Field A and for soybean in Field B (Figs. 1 and 2). In both corn and soybean, NDVI and LAI exhibited generally similar trends through the growing season. In corn, good relationships between NDVI and measured LAI were obtained for sites 101, 103, and 106 (Fig 1.) where a fully developed canopy was detected on the imagery. There was somewhat poorer agreement at site 102, where a significant amount of soil background was present in the image data as a result of a poor stand caused by surface runoff early in the growing season. Similarly, agreement was lower due to soil background at site 104, where problems with cultural operations during the season reduced stands. A decrease in NDVI was observed from day of year (DOY) 186 to 196 at each monitoring site. This was likely because the DOY 196 image was not radiometrically corrected, since tarps were not deployed on that date. NDVI was highest in the image taken on August 6 (DOY 218) and then dropped sharply for corn at all monitoring sites. More frequent image acquisition or field remote sensing with a handheld radiometer would be needed to more accurately determine the NDVI peak. Three dates of Landsat TM-derived NDVI

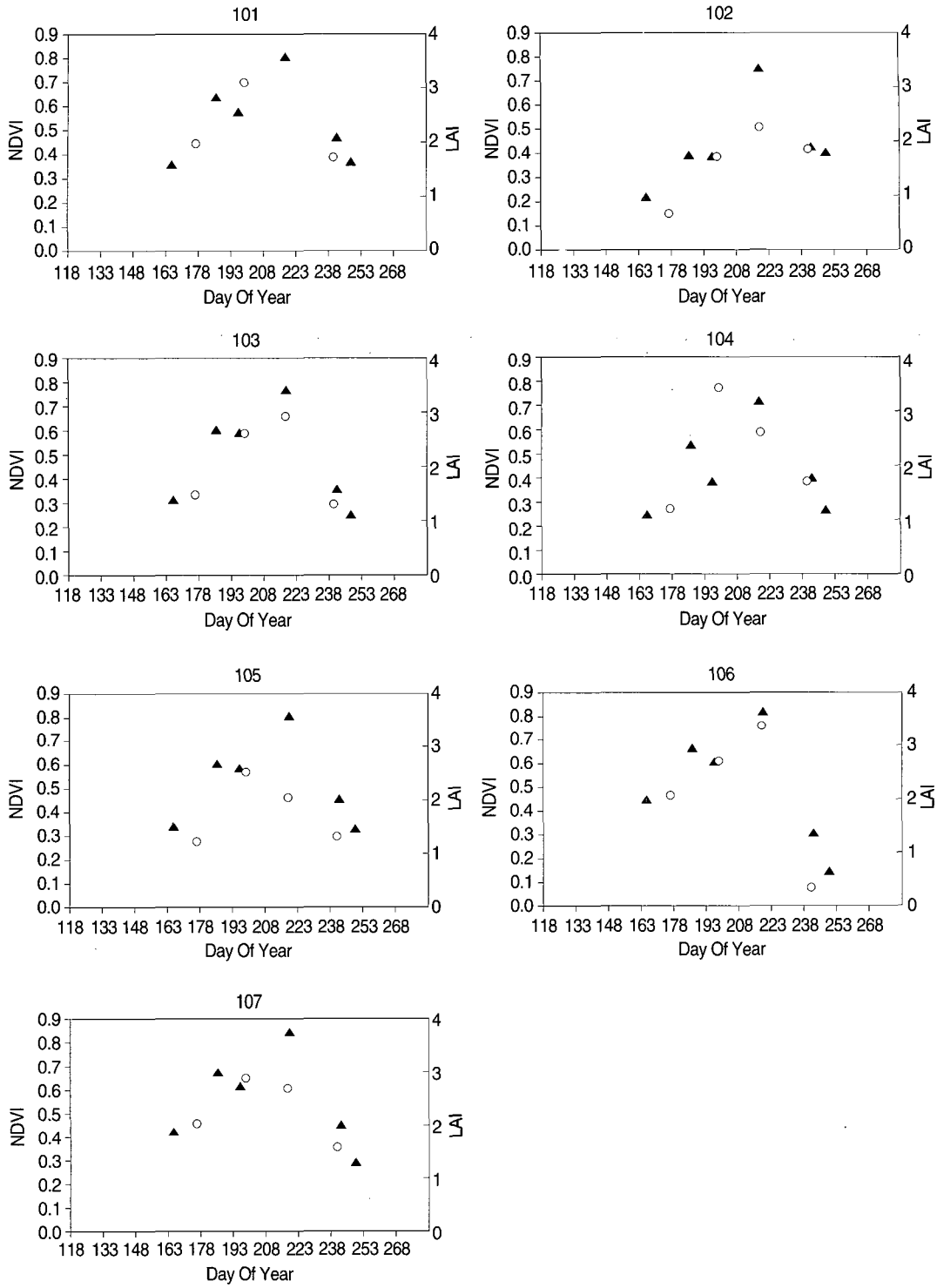

Fig. 1. Image-derived NDVI(▲) and LAI(○) of corn as a function of day of year for monitoring points 101-107 in Field A.

were compared with observed LAI and also exhibited good agreement for corn (data not shown). Regressions (Fig. 3) were developed to relate measured corn LAI to image-derived vegetation indices (NDVI, RVI, and SAVI) over the period of increasing LAI data (DOY 177 to 218).

Fig. 2 shows NDVI and measured LAI of soybean as a function of time for Field B. This no-till field was covered with crop residues and weeds at planting, although weeds were controlled by herbicide application six days prior to planting. NDVIs at all monitoring sites were similar, and ranged from 0.11 at DOY 186 to 0.88 at DOY 248. Up until about 20 days after flowering (R4 to R5, DOY 248), NDVIs in the monitoring sites were increasing. We assumed this occurred because soybean vegetative growth continued until approximately one month after flowering started, when maximum canopy stage was attained (Hong *et al.*, 2001), resulting in high NDVI values. Confirmation

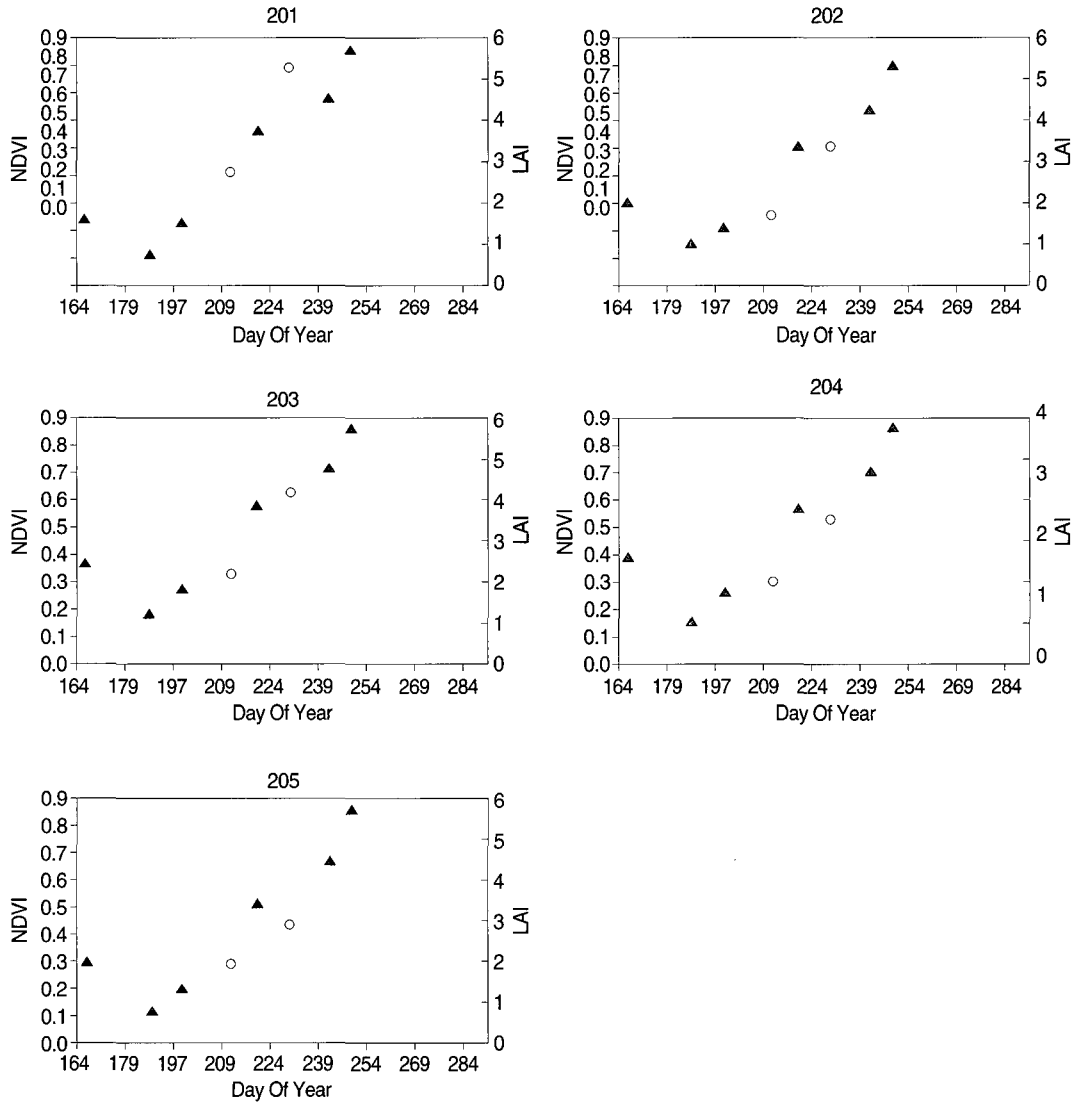

Fig. 2. Image-derived NDVI(▲) and LAI(○) of soybean as a function of day of year for monitoring points 201-205 in Field B.

of this assumption would require images to be obtained after maturation stage for estimating the peak VI. Soybean LAI was estimated from NDVI, RVI, and SAVI for the period from DOY 211 to 229, when observed LAI data were available (Fig. 3).

The best regressions relating LAI to VI were linear, with the exception of LAI versus RVI for corn, where a quadratic relationship provided a better fit. However, the LAI-RVI relationship for corn could be well-approximated by a linear equation for RVI values less than 5. Based on a comparison of r^2, there was very little difference in the quality of LAI estimations from various VIs (Fig. 3). Overall, NDVI estimates were slightly better across both crops, so NDVI-estimated LAI was used for comparison with model-simulated LAI.

2) Crop Simulation

The study fields received near-normal precipitation

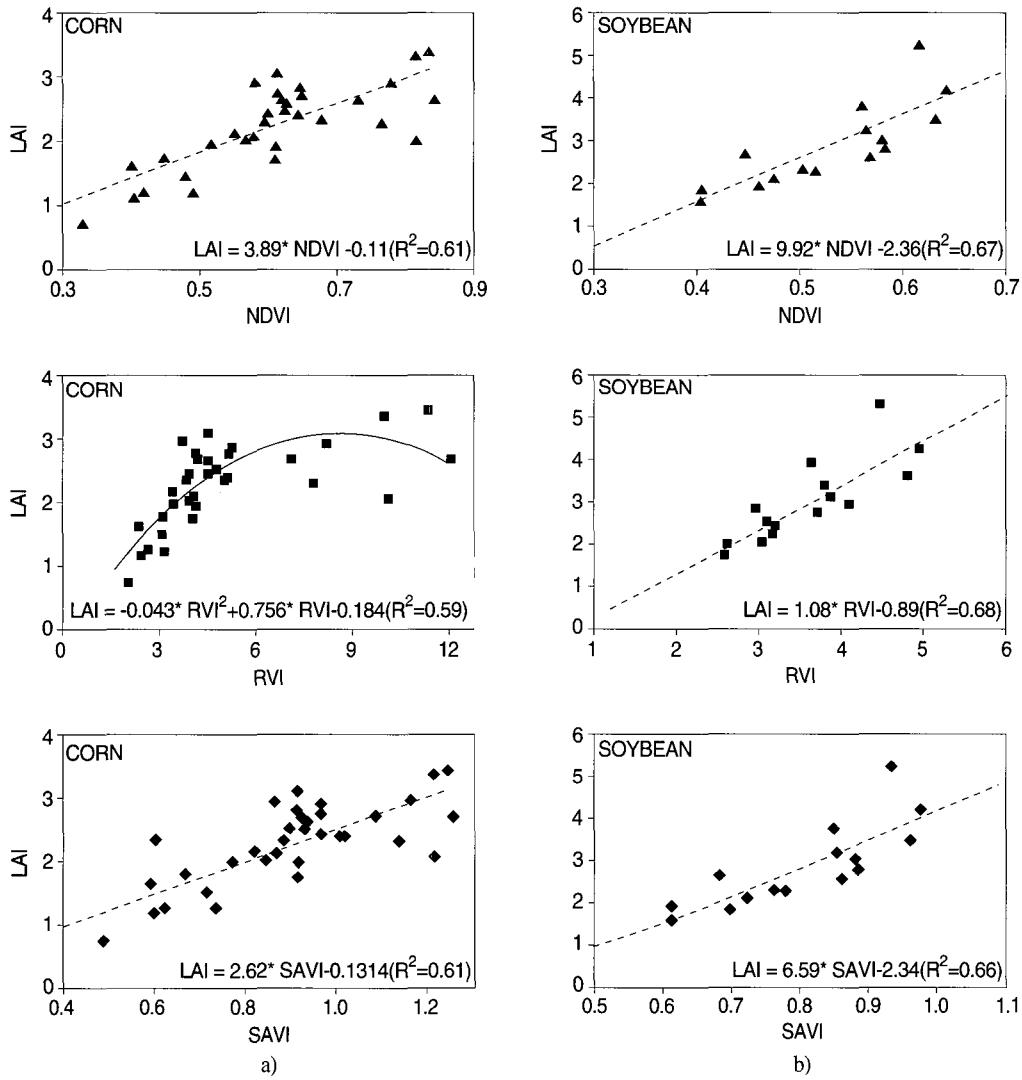

Fig. 3. LAI as a function of image-derived NDVI, RVI, and SAVI; a)for corn using data from June 26 to August 6, and b) for soybean using data from July 30 to August 17.

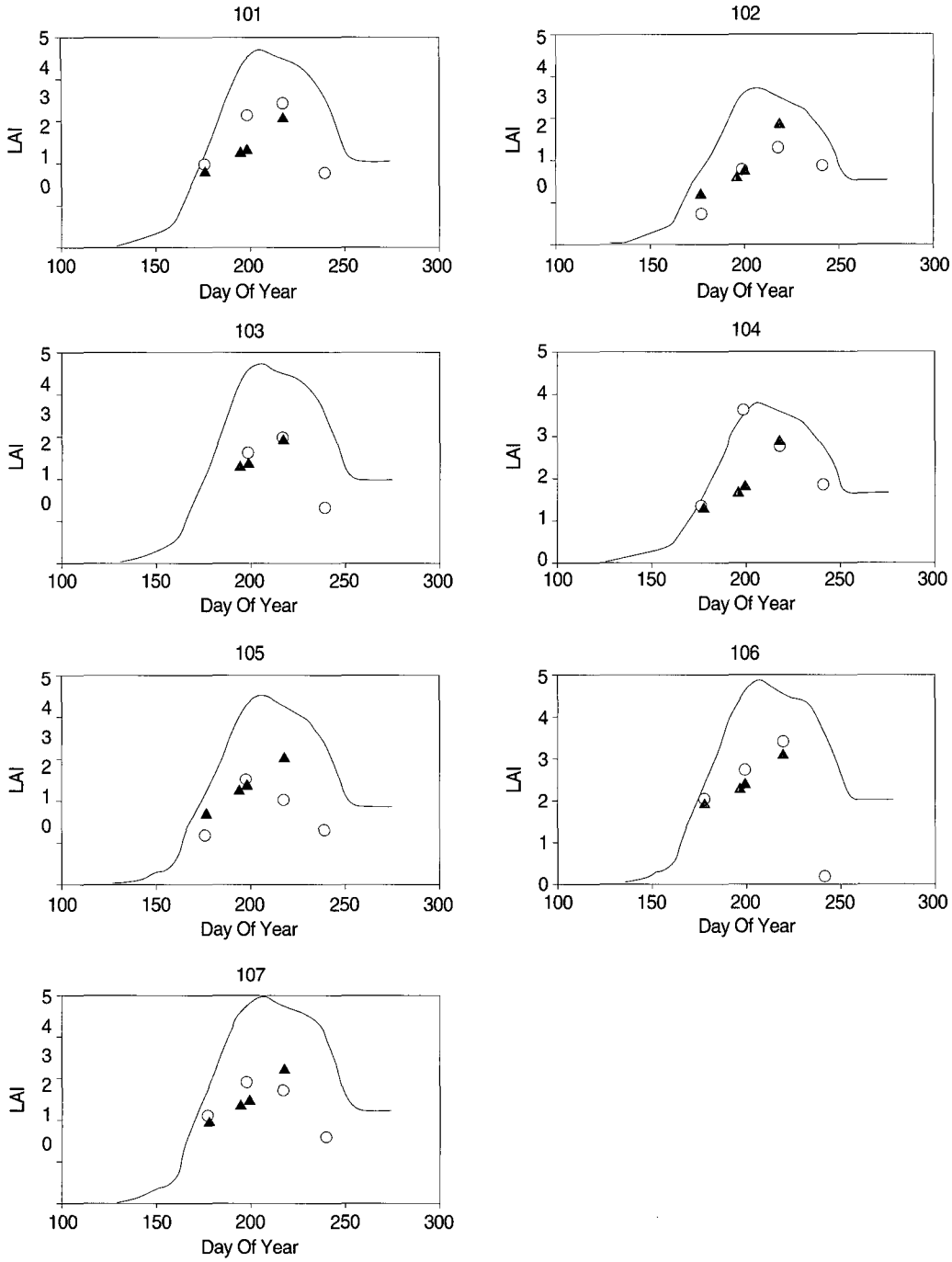

Fig. 4. Simulated(-), observed(○), and NDVI-estimated(▲) LAI for seven corn monitoring sites in Field A.

during the 2001 growing season. However, excess rain in the early spring caused ponding of water in depressional areas of Field A and excessive runoff in highly sloping areas. Within-field variation was high because of wet conditions and black cutworm pressure during the germination and emergence stages which

reduced corn stands in some locations. Crop simulation at site 102 was difficult due to poor stands caused by a wet early spring, a phenomenon also reported in previous years for this field (Fraisse *et al.*, 2001).

The CERES-Maize model was calibrated against measured soil moisture data (6 observations) and grain yield, and the simulated changes in LAI over the growing season were examined. LAI was significantly overestimated by the model at all monitoring sites (Fig. 4). Compared to results for the other sites, model-simulated LAI was low throughout the growing season for Sites 102 and 104, reflecting the poorer plant stand observed at these sites. These two locations also exhibited the lowest peak NDVI measurements of all sites. Sites 106 and 107 had the highest simulated peak LAI (Fig. 4) and NDVI values (Fig. 1). Thus, similar among-site trends were seen in both model-simulated LAI and in NDVI. However, LAI overestimation by the model, and the site-to-site variability in model fit, demonstrated two main challenges presented to modelers when simulating site-specific crop growth: 1) lack of knowledge to define specific genetic coefficients

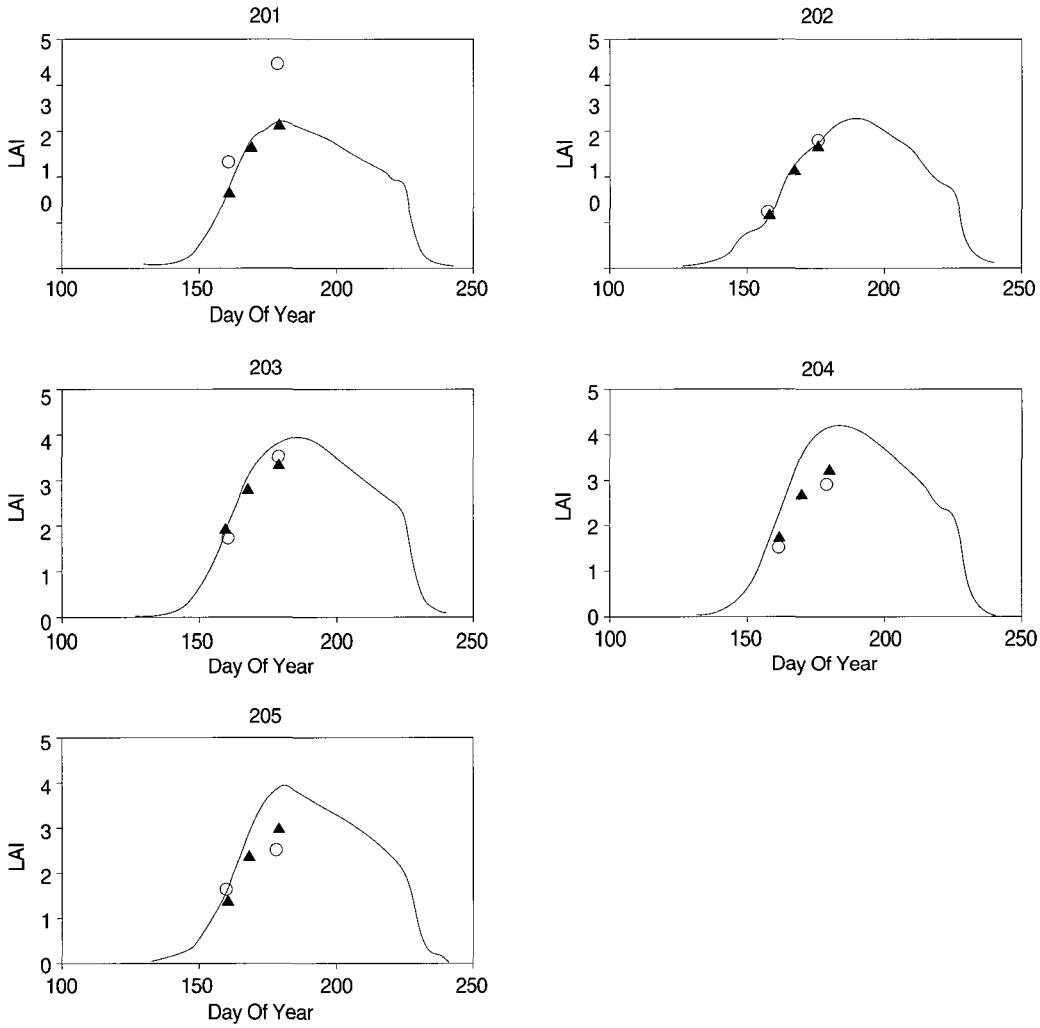

Fig. 5. Simulated(-), observed(○), and NDVI-estimated(▲) LAI for five soybean monitoring sites in Field B.

for the cultivar being simulated, and 2) lack of ability to deal with yield-limiting factors not taken into account by the model such as pests (e.g., black cutworm) and lateral water flow.

Soybean growing conditions were good at planting and during the maturing phases, generating good yield across the field. Fig. 5 shows the comparison between LAI simulated by the calibrated CROPGRO model, NDVI-estimated LAI, and observed LAI for the monitoring sites. Sites 202 and 203 showed good agreement between simulated, estimated and observed LAI. The highest yield was obtained in site 203, where topsoil is deeper and high yield has been observed in dry years. LAI was over-predicted by the model at sites 204 and 205 and under-predicted at site 201. However, the agreement among model-simulated, observed, and image-estimated LAI was much better for soybean than it was for corn.

3) Combining Remotely Sensed Data and Crop Models

The results of this study suggest that remotely sensed data might be useful to augment, and improve the results of, crop growth models. Although remote sensing can provide estimates of agronomic variables such as LAI with frequent observations at a fine spatial resolution over a whole field, remotely sensed data only gives an indirect indication of potential causes for the effects of any observed variability. Crop growth models can provide a more direct decision support system for explaining yield-limiting factors. Integration of crop growth models with remotely sensed information has been accomplished in several ways. According to Moulin *et al.* (1998), remote sensing observations can help extend the application of crop models to a regional scale by accounting for spatial variations of environmental conditions that affect crop growth and development without tedious ground surveys. They reviewed coupling methods for crop models and satellite data including: i) the forcing strategy that consists of updating at least one state variable using remote sensing data, ii) the re-initialization/re-parameterization approach, which consists of redefining model parameters or initial conditions to minimize the difference between a derived state variable or radiometric signal and its simulated value as determined by the crop model. Use of the forcing strategy for combining models and remote sensing data was evaluated by Barnes *et al.* (1997). They modified the CERES-Wheat model to accept remote sensing-derived LAI as an input variable and concluded that the approach would require further improvements in order to produce more accurate results. Basso *et al.* (2001) modified the CROPGRO-Soybean model to accept plant population and soil type as model inputs. Future work in this project should investigate the coupling of crop growth models and remotely sensed data for improved estimations of site-specific variation in crop growth and yield.

4. Conclusions

Image-derived vegetation indices and crop models were used to estimate and simulate LAI, and data were compared with measured LAI data for both corn and soybean. Over the growing season, the general trend in NDVI was similar to that in LAI. Measured LAI was expressed as a function of image-derived vegetation indices such as NDVI, RVI, and SAVI using LAI and image data taken from June 26 to August 6 for corn and from July 30 to August 17 for soybean. The quality of the LAI estimation was similar with all indices, and was likely reduced because the dataset included multiple sensors with different levels of radiometric calibration, different platforms, different spatial resolutions, and that encountered different amounts of atmosphere (i.e. airborne vs. satellite). Results might be improved by

using data from a single image provider, but that approach did not provide adequate temporal coverage for this study.

The CERES-Maize model was calibrated against measured soil moisture, LAI, and grain yield and over-predicted LAI in all monitoring sites. We assumed this was due to other yield-limiting factors that were not taken into account by the model, such as pests (i.e. black cutworm) and the impacts of early-season surface runoff on crop stand. The CROPGRO-Soybean model was well-calibrated against measured soil moisture, LAI, and grain yield. Generally good agreement was found between simulated and observed LAI in soybean, which had less variability in crop stand than did the corn. We suggest that remote sensing estimates of the spatial variability in LAI could be coupled with crop growth models for explaining yield variability within a field.

Acknowledgements

We thank the following for financial support or assistance enabling this research: Korean Government Long-Term Fellowship Program, North Central Soybean Research Program, United Soybean Board, Spectral Visions, NASA Scientific Data Purchase Program, and USDA-CSREES Special Water Quality Grants Program.

References

Baret, F. and G. Guyot, 1991. Potentials and limits of vegetation indices for LAI and APAR assessment, *Remote Sens. Environ.*, 35:161-173.

Barnes, E. M., P. J. Pinter Jr, B. A. Kimball, and G. W. Wall, 1997. Modification of CERES-Wheat to accept leaf area index as an input variable, *ASAE*, St. Joseph, MI. Paper No. 973016.

Basso, B., J. T. Ritchie, F. J. Pierce, R. P. Braga, and J. W. Jones, 2001. Spatial validation of crop models for precision agriculture, *Agr. Systems*, 68: 97-112.

Colvin, T. S., D. B. Jaynes, D. L. Karlen, D. A. Laird, and J. R. Ambuel, 1997. Yield variability within a central Iowa field, *Trans. ASAE*, 40: 883-889.

Donatelli, M., M. Acutis, and N. Laruccia, 1996. Evaluation of methods to estimate soil water content at field capacity and wilting point, *Proc. European Soc. Agronomy Congress*, Veldhoven, The Netherlands, pp.86-87,.

Doolittle, J. A., K. A. Sudduth, N. R. Kitchen, and S. J. Indorante, 1994. Estimating depths to claypans using electromagnetic induction methods, *J. Soil and Water Cons.*, 49(6): 572-575.

Fraisse, C. W., K. A. Sudduth, and N. R. Kitchen, 2001. Calibration of the CERES-Maize model for simulating site-specific crop development and yield on claypan soils, *Appl. Eng. Agric.*, 17(4): 547-556.

Green, A. A., M. Berman, P. Switzer, and M. D. Craig, 1988. A transformation for ordering multispectral data in terms of image quality with implications for noise removal, *IEEE Trans. on Geoscience and Remote Sensing*, 26(1): 65-74.

Hatfield, J. L., C. D. Stanley, and R. E. Carlson, 1976. Evaluation of an electronic foliometer to measure leaf area in corn and soybean, *Agron J.*, 68: 434-436.

Hong, S. Y., J. T. Lee, S. K. Rim, and J. S. Shin, 1997. Radiometric estimates of grain yields related to crop above-ground net production (ANP) in paddy rice, *Proc. IGARSS' 1997*, Singapore, pp.1793-1795.

Hong, S. Y., K. A. Sudduth, N. R. Kitchen, H. L. Palm, and W. J. Wiebold, 2001. Using hyperspectral remote sensing data to quantify within-field spatial variability, *Proc. 3rd Intl. Conf. on*

Geospatial Information in Agriculture and Forestry, Denver, CO., CD-ROM.

Hoogenboom, G., J. W. Jones, P. W. Wilkens, W. D. Batchelor, W. T. Bowen, L. A. Hunt, N. Pickering, U. Singh, D. C. Godwin, B. Baer, K. J. Boote, J. T. Ritchie, and J. W. White, 1994. Crop models, In: G. Y. Tsuji, G. Uehara, and S. Salas (eds.), *DSSAT v3*, 2(2). University of Hawaii, Honolulu, Hawaii.

Huete, A. R., 1988. A soil-adjusted vegetation index (SAVI), *Remote Sens. Environ.*, 25: 295-309.

Inoue, Y., 2001. Estimating eco-physiological crop variables based on remote sensing signatures and modeling, *Proc. NIAES-STA International Workshop 2001; Crop Monitoring and Prediction at Regional Scales*, Tsukuba, Japan.

Jones, C. A. and J. R. Kiniry, 1986. CERES-Maize: A *Simulation Model of Maize Growth and Development*, Texas A&M University Press, College Station, TX., pp.103-125.

Jordan, C. F., 1969. Derivation of leaf area index from quality of light on the forest floor, *Ecology*, 50: 663-666.

Kitchen, N. R., K. A. Sudduth, and S. T. Drummond, 1999. Soil electrical conductivity as a crop productivity measure for claypan soils, *J. Prod. Agric.*, 12(4): 607-617.

Maas, S. J., 1988. Using satellite data to improve model estimates of crop yield, *Agron. J.*, 80(4): 655-662.

Mao, C., 2000. Hyperspectral focal plane scanning - An innovative approach to airborne and laboratory pushbroom hyperspectral imaging, *Proc. of 2nd Intl. Conf. on Geospatial Information in Agriculture and Forestry*, Lake Buena Vista, FL., pp. I-424-428.

Matthews, R. B. and S. Blackmore, 1997. Using crop simulation models to determine optimum management practices in precision agriculture, *Proc. First European Conf. on Precision Agriculture*. Bios Scientific Publishers, Oxford, UK., pp.413-420.

Moulin, S., A. Bondeau, and R. Delecolle, 1998. Combining agricultural crop models and satellite observations: from field to regional scales, *Int. J. Remote Sensing*, 19(6): 1021-1036.

Rouse, J. W., R. H. Haas, J. A. Schell, and D. W. Deering, 1973. Monitoring vegetation systems in the great plains with ETRA, *Third ETRS Symposium, NASA SP-353*, U.S. Govt. Printing Office, Washington D.C., 1: 309-317.

Seidl, M .S., W. D. Batchelor, and J. O. Paz, 2002. Integrating remote images with crop models to improve spatial yield prediction for soybeans, *Trans. ASAE.*

Sudduth, K. A., S. T. Drummond, S. J. Birrell, and N. R. Kitchen, 1996. Analysis of spatial factors influencing crop yield, *Proc. 3rd Intl. Conf. on Precision Agriculture*, Madison, WI., American Society of Agronomy, LC. 129-140.

Sudduth, K. A., C. W. Fraisse, S. T. Drummond, and N. R. Kitchen, 1998. Integrating spatial data collection, modeling and analysis for precision agriculture, *Proc. First Intl. Conf. on Geospatial Information in Agriculture and Forestry*, Ann Arbor, MI., ERIM International, LC. 166-173.

Thenkabail, P. S., R. B. Smith, and E. D. Pauw, 2000. Hyperspectral vegetation indices and their relationships with agricultural crop characteristics, *Remote Sens. Environ.*, 71: 158-182.

Thomasson, J. A., R. Sui, M. S. Cox, and A. Al-Rajehy, 2001. Soil reflectance sensing for determining soil properties in precision agriculture, *Trans. ASAE*, 44(6): 1445-1453.

Wang, F., C. W. Fraisse, N. R. Kitchen, and K. A. Sudduth, 2002. Site-specific evaluation of the

CROPGRO-Soybean model on Missouri claypan soils, *Agricultural Systems*.

Watson, D. J., 1947. Comparative physiological studies on the growth of field crops: I. Variation in net assimilation rate and leaf area between species and varieties, and with and between years, *Ann. Bot.* (N.S.), 11: 41-76.

Wiegand, C. L., A. J. Richardson, R. D. Jackson, P. J. Pinter, Jr., J. K. Aase, D. E. Smika, L. F. Lautenschlager, and J. E. McMurtrey, III., 1986. Development of agrometeorological crop model inputs from remotely sensed information., *IEEE Trans. Geoscience and Remote Sensing*, 24(1): 90-97.

Wiegand, C. L., A. J. Richardson, D. E. Escobar, and A. H. Gerbermann, 1991. Vegetation indices in crop assessment, *Remote Sens. Environ.*, 35: 105-119.

Wood, G. A., J. C. Taylor, and R. J. Godwin, 2003. Calibration methodology for mapping within-field crop variability using remote sensing, *Biosystems Engineering*, 84(4): 409-423.